Electronic Supplementary Information

$3Pb_8O_7I_2 \cdot 2CsI$: Salt-inclusion strategy enriches the structural chemistry in lead oxyhalides

Mayinuer Maimaiti, [ab] Yuchen Yan, [b] Jinche Wu,[b] Tingwen Han, [b] Jing Xie*[a] and Min Zhang *[ab]

[a] State Key Laboratory of Chemistry and Utilization of Carbon Based Energy Resources, College of Chemistry, Xinjiang University, Urumqi 830017, Xinjiang, PR China.

[b] Research Center for Crystal Materials; State Key Laboratory of Functional Materials and Devices for Special Environmental Conditions; Xinjiang Key Laboratory of Functional Crystal Materials; Xinjiang Technical Institute of Physics and Chemistry, CAS, 40-1 South Beijing Road, Urumqi 830011, China.

*Corresponding author: zhangmin@ms.xjb.ac.cn; xiejing@xju.edu.cn.

Experimental Section

Reagents

Lead (II) oxide (PbO, 99.0%) lead (II) iodide (PbI_2, 98.0%) Cesium (II) iodide (CsI, 98.0%) were obtained from Aladdin Chemical Industry Co., Ltd. All materials were used as received.

Synthesis

$Cs_2Pb_{24}O_{21}I_8$

$Cs_2Pb_{24}O_{21}I_8$ single crystals were grown in a closed system high-temperature solution, reducing the volatilization of iodine at high temperatures. The synthesis processes are as follows: PbO (2.134g, 21 mol), CsI (0.237g, 2 mol), and PbI_2 (0.630g, 3 mol) were thoroughly ground mixtures and placed in 17mm (inner diameter) tubular corundum crucibles, and then the cover at the opening of the corundum crucible was sealed with a high-temperature resistant binder. The sealed corundum crucible was placed in a programmable constant temperature furnace, gradually heated to 560-600 ˚C, and kept at this temperature to ensure the uniformity of the solution, the temperature was cooled to 300 ˚C at a rate of 1 ˚C h^{-1}, then cooled to 50 ˚C at a rate of 2 ˚C h^{-1}, and then the furnace is closed. After reactions, better crystals were manually picked under an optical microscope for structural determination.

The synthesis process of the $Cs_2Pb_{24}O_{21}I_8$ polycrystalline sample is as follows: CsI (2mol, 0.037g), PbO (21mol, 0.332g), and PbI_2 (4mol, 0.131g) with a molar ratio of 2: 21: 4 was fully ground and mixed in an agate mortar and transferred into a quartz tube, and the quartz tube was sealed with a hydrogen-oxygen flame in a vacuum environment (10^4 Pa). The sealed tube was then placed in a single crystal furnace for slow heating to 485 ˚C and kept at this temperature for 20 hours, then rapidly cooling to room temperature. The purity of the samples was examined by powder XRD diffraction.

$Pb_8O_7I_2$

The $Pb_8O_7I_2$ compound was reported by D.O.Charkin et al. in 2022,[1] but only the structural composition was described, and the characterization of optical and thermodynamic properties was lacking. Herein, the single crystal of $Pb_8O_7I_2$ was obtained again by using the high-temperature solution method. The reactants with a molar ratio of PbO: PbI_2 = 7: 1 were fully ground, mixed in an agate mortar, and then placed in a 17 mm (inner diameter) tubular corundum crucible. The lid at the opening of the corundum crucible was sealed with a high-temperature-resistant binder. The sealed corundum crucible was placed in a programmable constant temperature furnace, gradually heated to 560-600 ˚C, and kept at this temperature to ensure the uniformity of the solution. Then it was cooled to 300 ˚C at a rate of 1 ˚C h^{-1}, then slowly cooled to 200 ˚C at a rate of 2 ˚C h^{-1}, and then the furnace was closed. The best crystals are manually picked under a light microscope for structural determination.

The powder sample of $Pb_8O_7I_2$ can be fully ground by a mixture of PbO and PbI_2 at a ratio of 7: 2 in agate mortar and moved into an opening porcelain crucible, and then placed in a single crystal furnace for slow heating to 320 ˚C and maintained at this temperature for 20 hours, followed by rapidly cooling to room temperature. The purity of the sample was examined by powder XRD diffraction.

Single crystal X-ray diffraction

A high-quality transparent single crystal was used for the data collection. The crystal structure of $Cs_2Pb_{24}O_{21}I_8$ was determined at room temperature on a Bruker D8 Venture single-crystal X-ray diffractometer using the Mo-Kα radiation (λ = 0.71073 Å). Numerical absorption corrections were

carried out using the SCALE program for the area detector and integrated with the SAINT program.[2] Then, the crystal structure was solved by direct methods and refined using the SHELXTL crystallographic software package.[3-4] All atoms were refined with anisotropic displacement parameters. The program PLATON was used for verifying the possible missing symmetry elements,[5] but no higher symmetries were found. Finally, the crystal structure of $Cs_2Pb_{24}O_{21}I_8$ was confirmed. Table S1 presents the crystal data and structure refinements of the compound. The atomic coordinates, bond valence sum (BVS) calculations, bond distances and angles, and isotropic displacement parameters are presented in Tables S2-3.

Powder X-ray diffraction

The purity of the synthesized $Cs_2Pb_{24}O_{21}I_8$ and $Pb_8O_7I_2$ polycrystalline samples was verified by powder X-ray diffraction (PXRD), using a Bruker D2 Phaser diffractometer equipped with a diffracted beam monochromator set for Cu-Kα radiation (λ = 1.5418 Å). The PXRD pattern was recorded from 5˚ to 70˚ (2θ) with a scan step width of 0.01˚ and a fixed counting time of 1s per step.

Thermal analysis

Thermal gravimetric analysis (TGA) and differential scanning calorimetry (DSC) were measured on a simultaneous NETZSCH STA 449F3 thermal analyzer instrument at a temperature range of 40-850 ˚C with a heating rate of 5 ˚C /min in an atmosphere of flowing N_2.

Infrared (IR) spectroscopy

The Infrared spectrum was recorded with a Shimadzu IR Affinity-1 Fourier transform infrared spectrometer in the range of 400-4000 cm^{-1} with a resolution of 2 cm^{-1}. The samples for measurement were prepared by pressing a thoroughly ground mixture of pure powder sample and dried KBr with a ratio of about 1: 200.

UV–Vis–NIR diffuse reflectance spectroscopy

The diffuse reflectance spectrum of the $Cs_2Pb_{24}O_{21}I_8$ and $Pb_8O_7I_2$ powder sample in the 210-2600 nm was measured using a Shimadzu Solid Spec-3700 DUV spectrophotometer at room temperature.

Calculation details

The target compound's electronic structures and optical properties were performed based on the density functional theory (DFT) method implemented in the CASTEP package.[6-7] The exchange-correlation potential was treated by the Perdew-Burke-Ernzerh (PBE) of method in the generalized gradient approximation (GGA) and the interactions between the ionic cores and electrons were described by norm-conserving pseudopotential (NCP), the following orbital electrons were treated as valence electrons: Cs $5s^2$ $5p^6$ $6s^1$, Pb $6s^2$ $6p^2$, O $2s^2$ $2p^4$, and I $5s^2$ $5p^5$ in the calculations. The kinetic energy cutoffs of 750 eV and 1 × 1 × 2 were chosen, and Monkhorst-Pack k-point meshes spanning 0.05/Å in the Brillouin zone.[8]

Table S1. Crystal data and structure refinement for $Cs_2Pb_{24}O_{21}I_8$ and $Pb_8O_7I_2$.

Empirical formula	$Pb_8O_7I_2$	$Cs_2Pb_{24}O_{21}I_8$
Formula weight	2023.320	6590.239
Temperature(K)	303.0	302.0
Wavelength (Å)	0.71073	0.71073
Crystal system, space group	Monoclinic, $P2_1/m$	Tetragonal, $P4_2/n$
Unit cell dimensions	a=9.1468(5) Å, α= 90° b=21.3363(15) Å, β=110.429(2)° c=12.9275(9) (Å), γ=90°	a=17.3092(4) Å, α= 90° b=17.3092(4) Å, β= 90° c=9.1504(3) (Å), γ= 90°
Volume(Å^3)	2364.2(3)	2741.54(13)
Z, Density calculated (Mg.m^{-3})	6, 8.527	2, 7.983
Absorption coefficient (mm^{-1})	89.049	79.250
F (000)	4908.0	5210.8
Crystal size/mm3	0.154 × 0.146 × 0.089	0.167 × 0.142 × 0.094
Theta range for data collection	1.681 to 27.514°	2.35 to 25.03°
Index ranges	-10 ≤ h ≤ 11, -25 ≤ k ≤ 27, -16 ≤ l ≤ 16	-22 ≤ h ≤ 22, -22 ≤ k ≤ 22, -11 ≤ l ≤ 11
Reflections collected/unique	24185/5570 [R(int)= 0.0793]	35266/2410 [R(int)= 0.0978]
Completeness (%)	99.8	99.9
Data/restraints/parameters	5570/12/248	2410/6/125
Goodness-of-fit on F^2	0.964	0.986
Final R indexes [Fo^2>=2σ(Fo^2)] [a]	R1 = 0.0344, wR2 = 0.0634	R1= 0.0230, wR2= 0.0490
R indexes [all data] [a]	R1 = 0.0543, wR2 = 0.0695	R1= 0.0313, wR2= 0.0537
Largest diff. peak and hole	2.53 and -2.74 e·Å^{-3}	1.58 and -1.48 e·Å^{-3}

[a]$R1 = \Sigma||Fo| - |Fc||/\Sigma|Fo|$ and $wR2 = [\Sigma w(Fo^2 - Fc^2)^2 / \Sigma wFo^4]^{1/2}$ for $Fo^2 > 2\sigma(Fo^2)$

Table S2. Fractional atomic coordinates (×10^4), equivalent isotropic displacement parameters(Å^2×10^3), and bond valence sum (BVS) for $Cs_2Pb_{24}O_{21}I_8$. U(eq) is defined as one-third of the trace of the orthogonalized Uij tensor.

Atoms	Wyckoff	x	y	z	U(eq)	BVS[a)]
Cs(1)	4e	2500	7500	1380.4(10)	31.6(3)	0.97
Pb(1)	8g	786.3(2)	4443.6(2)	6707.2(4)	17.09(11)	2.24
Pb(2)	8g	2192.9(2)	3533.4(2)	8987.3(4)	16.93(10)	2.10
Pb(3)	8g	2879.8(2)	5084.8(2)	6754.1(4)	17.38(11)	2.25
Pb(4)	8g	4446.3(2)	4319.0(2)	3915.4(4)	14.63(10)	2.32
Pb(5)	8g	2139.5(2)	3735.5(2)	3396.7(4)	17.52(11)	1.91
Pb(6)	8g	2949.1(2)	5142.2(2)	1063.3(4)	15.28(10)	2.30
O(1)	8g	513(4)	3187(4)	6048(6)	15.8(15)	2.28
O(2)	8g	2005(4)	4163(4)	6852(6)	17.3(16)	2.32
O(3)	8g	2005(4)	4163(4)	6852(6)	17.3(16)	2.22
O(4)	8g	3401(4)	4172(4)	2475(7)	18.3(16)	2.13
O(5)	2a	2500	2500	2500	20(3)	1.96
O(6)	8g	1971(4)	4271(4)	1094(6)	12.2(14)	2.46
I(1)	8g	1520.1(4)	5789.5(5)	3824.7(7)	26.77(18)	0.79
I(2)	8g	1443.3(4)	6049.5(4)	-1094.9(7)	23.04(17)	1.02

a) The bond valence sum is calculated by bond-valence theory (Sij = exp[(R0-R)/B, where R is an empirical constant, R_0 is the length of bond I (in angstroms), and B= 0.37).

Table S3. Selected bond lengths (Å) and angles (°) for $Cs_2Pb_{24}O_{21}I_8$.

Cs(1)-I(1)	4.0800(9)	Pb(3)#6-O(1)-Pb(2)#6	98.9(2)
Cs(1)-I(3)	4.0800(9)	Pb(6)#11-O(1)-Pb(1)	119.6(3)
Cs(1)-I(1)#1	4.1367(9)	Pb(6)#11-O(1)-Pb(2)#6	101.7(2)
Cs(1)-I(1)#2	4.1367(9)	Pb(6)#11-O(1)-Pb(3)#6	118.1(3)
Cs(1)-I(2)#4	3.8712(9)	Pb(2)-O(2)-Pb(1)	107.5(3)
Cs(1)-I(2)#5	3.8712(9)	Pb(3)-O(2)-Pb(1)	120.3(3)
Cs(1)-I(2)#3	3.8443(9)	Pb(3)-O(2)-Pb(2)	106.6(3)
Cs(1)-I(2)	3.8443(9)	Pb(2)#8-O(3)-Pb(1)#8	96.9(2)
Pb(1)-O(1)	2.307(7)	Pb(3)-O(3)-Pb(1)#8	94.6(2)
Pb(1)-O(2)	2.169(7)	Pb(3)-O(3)-Pb(2)#8	121.5(3)
Pb(1)-O(3)#6	2.320(6)	Pb(4)-O(3)-Pb(1)#8	122.1(3)
Pb(2)-O(1)#8	2.384(7)	Pb(4)-O(3)-Pb(2)#8	99.8(2)
Pb(2)-O(2)	2.260(6)	Pb(4)-O(3)-Pb(3)	121.0(3)
Pb(2)-O(3)#6	2.453(7)	Pb(5)-O(4)-Pb(4)	123.2(3)
Pb(2)-O(6)#7	2.343(6)	Pb(5)#10-O(4)-Pb(4)	96.0(2)
Pb(3)-O(1)#8	2.324(6)	Pb(6)-O(4)-Pb(4)	121.9(3)
Pb(3)-O(2)	2.202(7)	Pb(6)-O(4)-Pb(5)	96.7(2)
Pb(3)-O(3)	2.312(6)	Pb(6)-O(4)-Pb(5)#10	125.3(3)
Pb(4)-O(3)	2.263(6)	Pb(5)-O(5)-Pb(5)#11	96.861(6)
Pb(4)-O(4)	2.253(7)	Pb(5)#10-O(5)-Pb(5)	96.861(6)
Pb(4)-O(6)#10	2.253(6)	Pb(5)#10-O(5)-Pb(5)#11	139.561(17)
Pb(5)-O(4)#11	2.475(7)	Pb(5)#13-O(5)-Pb(5)#11	96.861(6)
Pb(5)-O(4)	2.460(7)	Pb(5)#13-O(5)-Pb(5)	139.561(17)
Pb(5)-O(5)#10	2.3741(4)	Pb(5)#10-O(5)-Pb(5)#13	96.861(6)
Pb(5)-O(6)	2.320(6)	Pb(4)#11-O(6)-Pb(2)#12	103.5(2)
Pb(6)-O(1)#10	2.278(6)	Pb(5)-O(6)-Pb(2)#12	120.6(3)
Pb(6)-O(4)	2.259(6)	Pb(5)-O(6)-Pb(4)#11	100.5(2)
Pb(6)-O(6)	2.269(6)	Pb(6)-O(6)-Pb(2)#12	103.3(2)
		Pb(6)-O(6)-Pb(4)#11	130.5(3)
Pb(2)#6-O(1)-Pb(1)	122.9(3)	Pb(6)-O(6)-Pb(5)	100.5(2)
Pb(3)#6-O(1)-Pb(1)	94.6(2)		

Symmetry transformations used to generate equivalent atoms:

#1 1/2+Y,1-X,1/2+Z; #4 1-Y,1/2+X,1/2+Z; #7 +X,+Y,1+Z;

#2 -Y,1/2+X,-1/2+Z; #5 -1/2+Y,1-X,1/2+Z; #8 +Y,1/2-X,3/2-Z;

#3 1/2-X,3/2-Y,+Z; #6 1/2-Y,+X,3/2-Z; #9 1-X,1-Y,1-Z;

#10 +Y,1/2-X, 1/2-Z; #11 1/2-Y,+X,1/2-Z.

Figure S1. The coordination environments of Pb in the crystal structure of $Cs_2Pb_{24}O_{21}I_8$

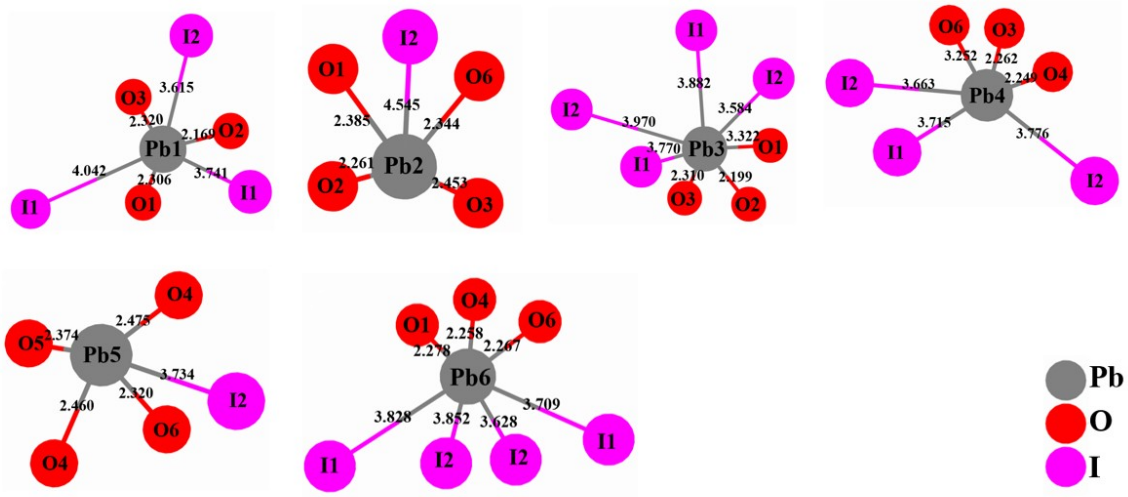

Figure S2. The coordination environments of Pb in the crystal structure of $Pb_8O_7I_2$

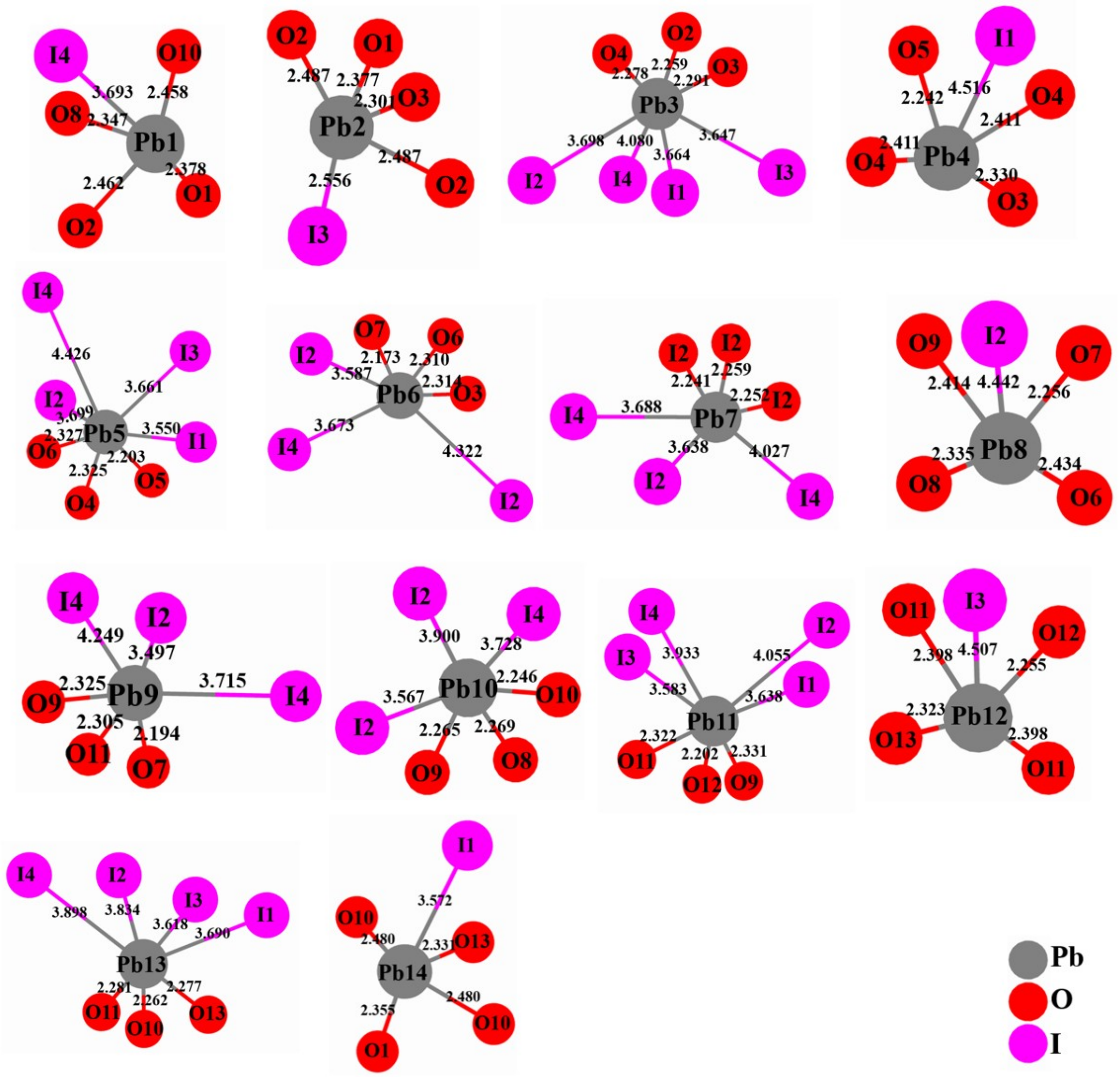

Figure S3. The statistics of Pb-O-Pb angles (˚) and Pb-Pb bond distance (Å) in the crystal structure of lead oxyhalide compounds.

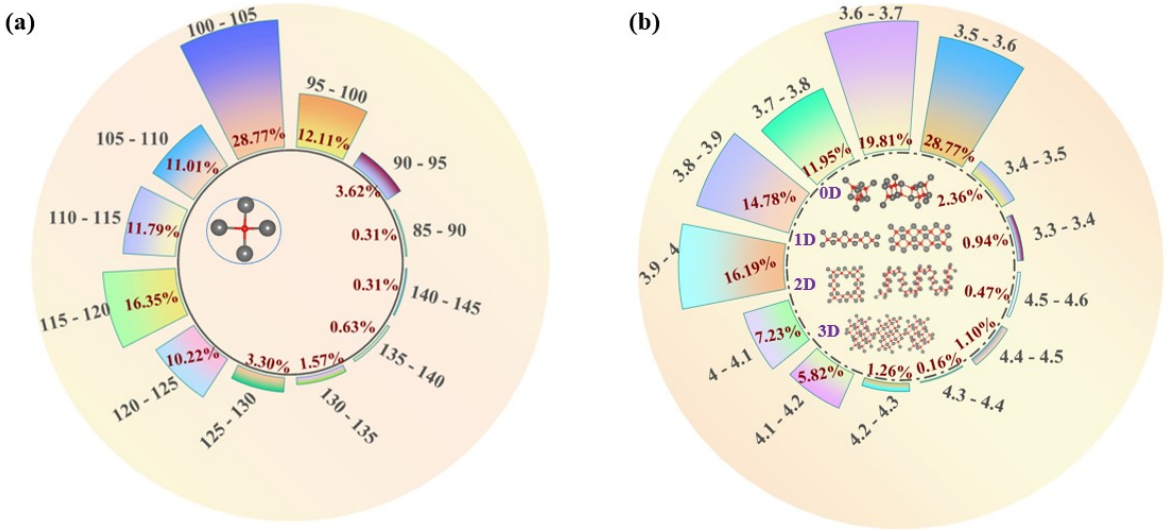

Angles of O-Pb-O (°) **Distances of Pb-Pb (Å)**

Figure S4. The experimental and calculated powder XRD patterns (a), the TG-DSC curves and UV-Vis-NIR diffuse reflectance spectrum (b and c, respectively), and the IR spectrum(d) of $Pb_8O_7I_2$.

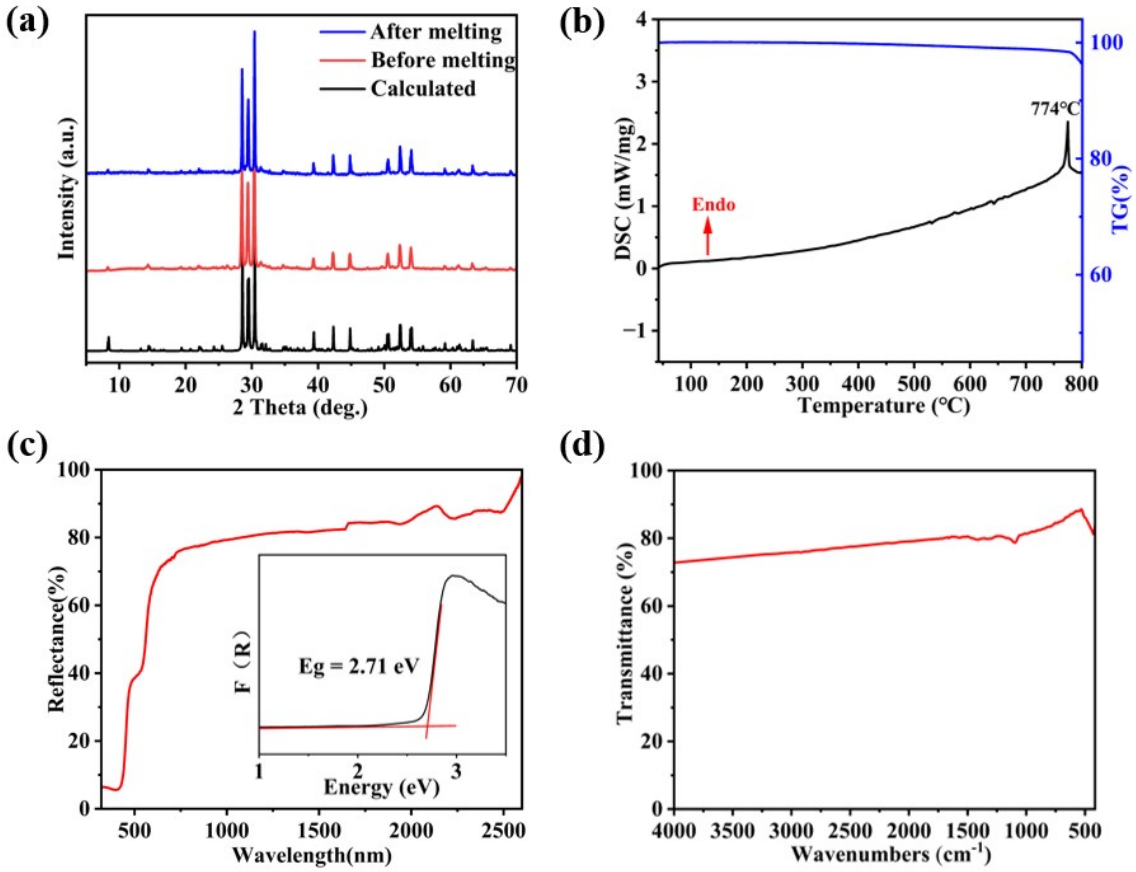

References

1. D. O. Charkin, A. S. Borisov, V. E. Kireev, A. N. Kuznetsov, S. Umedov, E. V. Nazarchuk, V. N. Bocharov and O. I. Siidra, *J. Solid State Chem.*, 2022, **312**, 123277.
2. V. SAINT, *Inc., Madison, WI.*, 2008.
3. O. V. Dolomanov, L. J. Bourhis, R. J. Gildea, J. A. K. Howard and H. Puschmann, *J. Appl. Crystallogr.*, 2009, **42**, 339-341.
4. G. M. Sheldrick, *Acta Cryst C.*, 2015, **71**, 3-8.
5. A. L. Spek, *J. Appl. Crystallogr.*, 2003, 36, 7-13.
6. S. J. Clark, M. D. Segall, C. J. Pickard, P. J. Hasnip, M. I. J. Probert, K. Refson and M. C. Payne, *Z. Krist. Cryst. Mater.*, 2005, **220**, 567-570.
7. L. J. Sham and M. Schlüter, *Phys. Rev. Lett.*, 1983, **51**, 1888-1891.
8. H. J. Monkhorst and J. D. Pack, *Phys Rev* B., 1976, **13**, 5188-5192.